Preliminary analysis of a new high lift device for sailing cargo ships using distributed wing-mounted propellers

Sergio E. Perez, Department of Marine Engineering, U.S. Merchant Marine Academy, Kings Point, NY, perezs@usmma.edu

ABSTRACT/CONCLUSIONS

This work is a preliminary analysis of a novel method of generating large lift forces from rigid wing-sails on cargo ships under wind-assisted propulsion. The propeller sail, consisting of powered propellers placed spanwise on the trailing edge of wing-sails, can prevent separation at high sail angles of attack, permitting lift coefficients several times greater than un-assisted sails, and of similar magnitude to other high-lift devices such as Flettner rotors and suction sails.

1) Mounting propellers on the aft end of a NACA 0030 rigid wing-sail at 30 degrees angle of attack appears to produce lift coefficients of 5 and higher.
2) Increasing the propeller exit speed increases the coefficient of lift, with a small increase in drag and an increase in required power.
3) A combination of propeller and flap on the wing produced the highest lift coefficient of all configurations tested, with a very large increase in drag force. A better option may be the wing and propeller without the flap, which has a lift coefficient not too far below that of the propeller and flap, but with a much lower drag coefficient.
4) Placing the propeller on the aft end of the wing produces somewhat less lift, but considerably less drag than mounting the propellers forward of the wing.
5) Induced drag is the Achilles heel of high lift devices when applied to low aspect ratio sails. Contra-vortex wingtip propellers (spinning in a direction opposite to that of the vortices normally shed by wings and sails) may significantly reduce the induced drag on the propeller sail, as well as on Flettner rotors and suction sails. Wing sails should be mounted flush with the deck to further reduce induced drag.
6) Based on the preliminary analysis conducted here, the use of propeller sails on a 15,000 CDWT cargo vessel moving in light winds could result in significant fuel savings.
7) The results of this work must be verified by further research.

Introduction

In this preliminary work, we analyze the lift and drag characteristics of a NACA 0030 wing sail with a series of powered, distributed propellers at the trailing edge of the wing. The purpose of the propellers is to prevent flow separation at high angles of attack, by providing suction. If separation can be reduced, wings can be used at higher angles of attack, which permits higher lift forces. In addition, if the propellers on the wingtips spin in a direction opposite to that of the vortices shed by the wing, the induced drag on the sail wings can be greatly reduced. High drag is a problem that can affect all high lift devices, especially those with low aspect ratios, where the sails/wings are relatively short in height. Figure 1 shows the propeller sail concept using low aspect ratio wings.

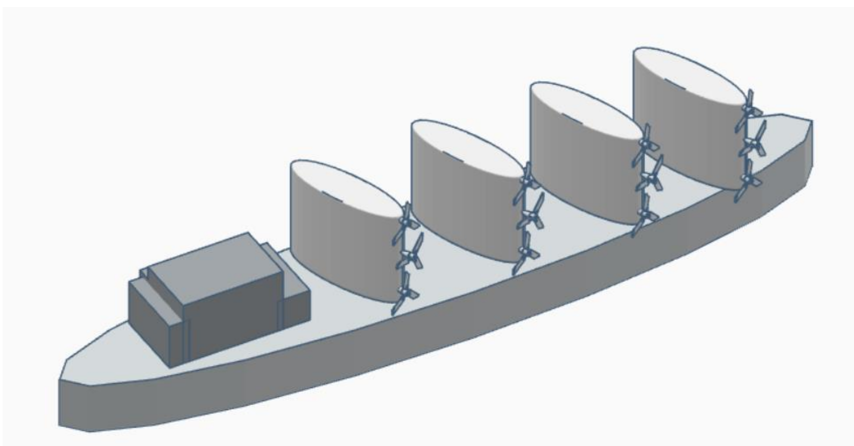

Figure 1. The propeller sail concept, mounted on low aspect ratio wings. The vessel's bow is on the left, with wind from the vessel's starboard side.

It was calculated [1], that a 45,000 CDWT cargo ship using sail power as the primary means of propulsion would require a mast height of 92 m (302 ft). However, the use of such high masts would significantly reduce the number of ports such a vessel could access, and until infrastructure changes can be made, shipping will be more likely to use wind energy to assist engines rather than to serve as the prime motive power, which will require sails to be as small as possible.

One solution is the use of sail "high-lift devices", which would permit the use of smaller sails. These include wing flaps and slats as used on aircraft [2], Flettner rotors [3] and suction sails (also referred to as ventifoils and turbosails) [4], as well as the propeller sails discussed in this report.

The Propeller Sail

It is well-known that separation occurs in flows when strong adverse pressure gradients are encountered. Figure 2 shows a CFD (Computational Fluid Dynamics) simulation of flow over a cylinder. As the flow moves from left to right over the cylinder, it separates from the cylinder surface near the cylinder's widest portion.

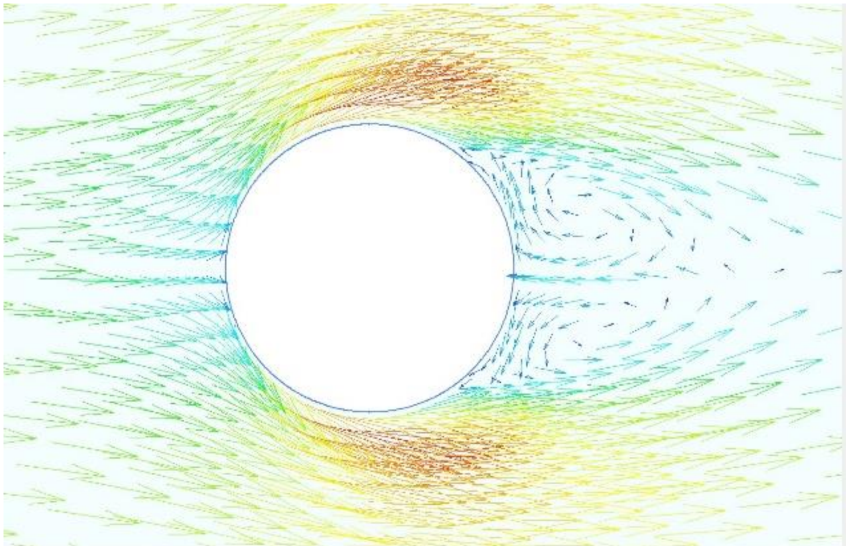

Figure 2. Flow separation over a cylinder

The flow in Figure 2 is seen to accelerate as it moves over the cylinder (red represents the fastest speed), reaching a maximum speed of about twice the upstream velocity at the widest portion of the cylinder. The increasing speed over the leading edge of the cylinder is accompanied by a decreasing pressure. The pressure gradient on the leading edge of the cylinder is said to be favorable, because pressure is dropping ahead of the flow's path. Beyond the widest portion, the flow velocity along the surface of the cylinder decreases, accompanied by increasing pressure. This increasing pressure is referred to as an adverse pressure gradient, and is analogous to a ball rolling uphill. Due to friction, the flow has lost energy, and is not able to penetrate fully though the adverse gradient. The flow then separates or detaches from the surface of the cylinder.

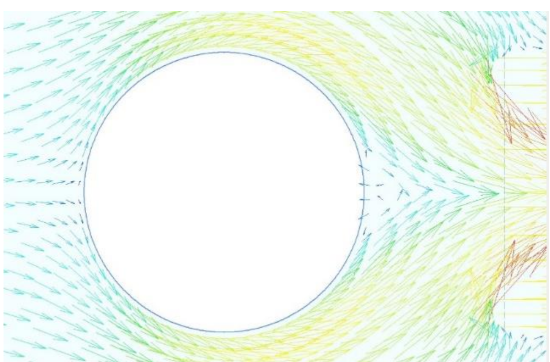

Figure 3 Flow around a cylinder with a propeller accelerating flow to the right. The propeller is seen as a thin, dashed vertical line behind the cylinder. Separation is greatly reduced.

Figure 3 shows a cylinder again, but with a propeller providing suction aft. The propeller in this case is accelerating the flow into the propeller, providing a suction which tends to pull the flow over the cylinder, greatly reducing the separation. (In the simulations performed in this work using computational fluid dynamics (CFD), a true propeller is not used, rather an actuator disk that increases the linear speed of the flow through the disk, in the same way as a propeller but without the added rotation). The flow is seen to remain attached for substantially longer.

Figure 4 shows a 2-dimensional CFD (Computational Fluid Dynamics) simulation of flow around a 1m-long NACA 0030 airfoil (selected because thicker airfoils with large leading-edge radii are known to resist separation more effectively than thinner ones [2]). The airfoil is inclined at an angle of attack of 30 degrees to 7.2 m/s airflow.

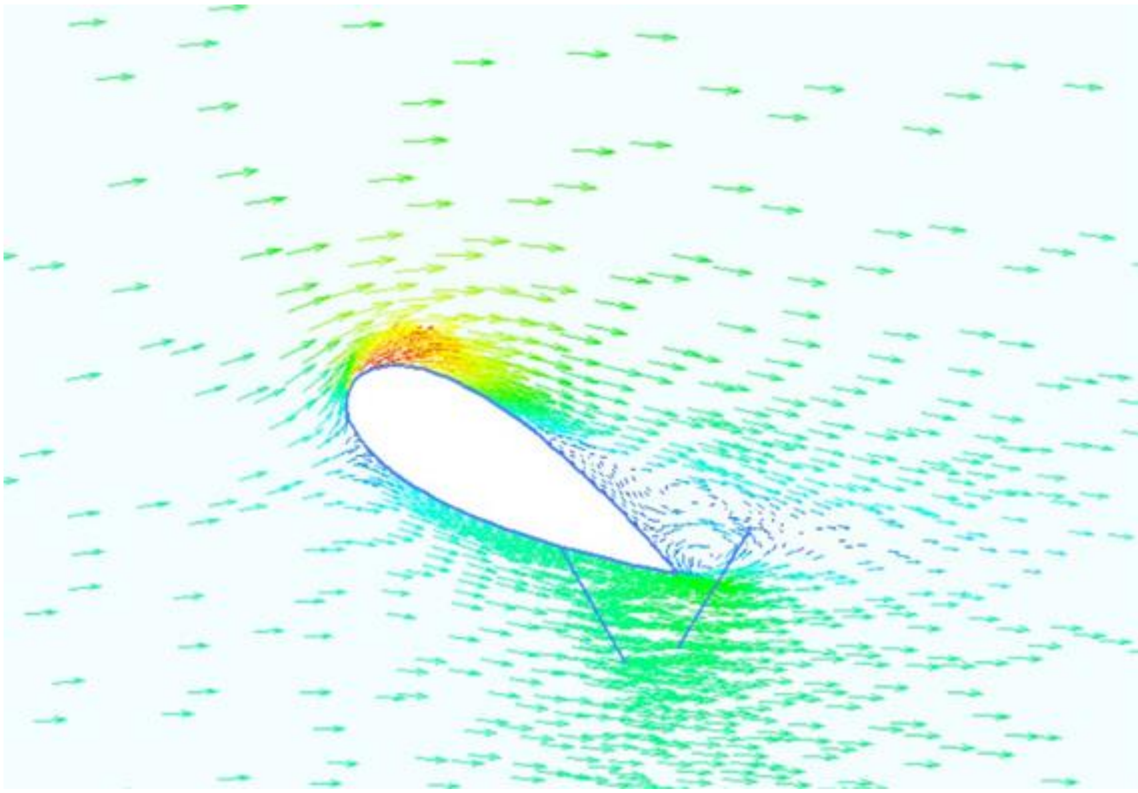

Figure 4. Flow over NACA 0030 airfoil without propeller suction. Separation is seen around mid-way on the suction side (top) of the airfoil. The flap and propeller at the rear of the airfoil are pictured to indicate their positions. They have no effect upon the flow on this CFD run.

As with the cylinder, the flow accelerates around the leading edge of the airfoil with a favorable pressure gradient and reaches a maximum velocity, as shown by the red arrows. The flow then experiences decreasing velocity/increasing pressure as it continues its path along the wing, and the flow detaches from the body at about mid-chord (the linear distance between leading and trailing edges of an airfoil is referred to as the chord). Once separated, the flow moves in a clockwise circulation similar to that displayed by the cylinder. Due to flow separation, the airfoil produces high drag forces with diminished lift forces.

Figure 5 shows the effect of activating the propeller with 10 m/s exit speed, on the same airfoil seen in Figure 4. One can see separation is reduced, and the flow leaving the wing has a greater downward component.

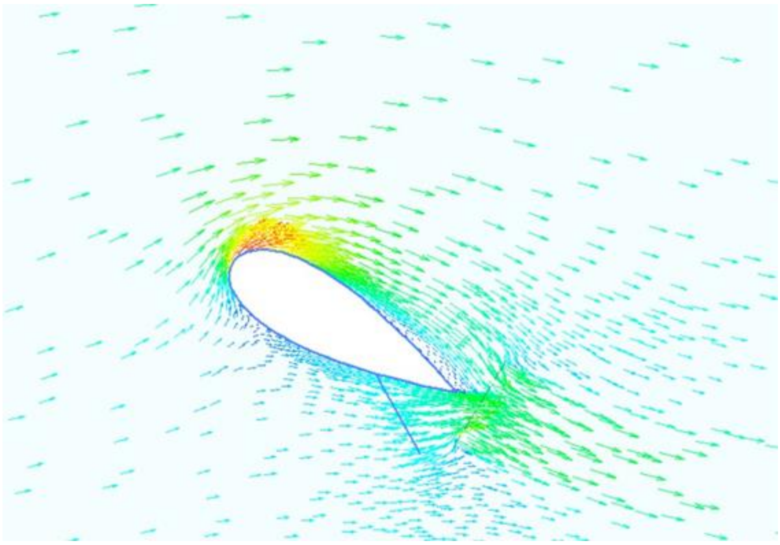

Figure 5. The NACA 0030 section with propeller suction applied. Separation is substantially reduced.

Figure 6 shows the effect of activating the flap and propeller in unison. Separation is further decreased, and the flap directs more flow downwards. Also noted is the large separation area behind the flap, which must increase total drag forces.

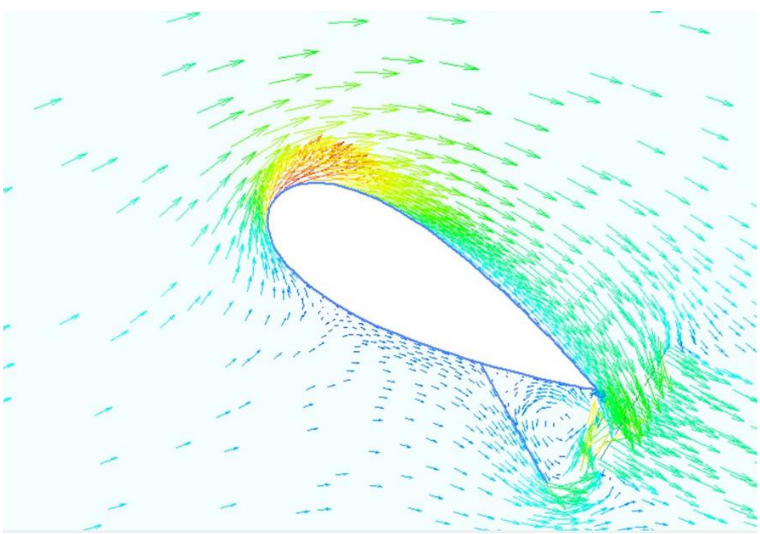

Figure 6. The flap and propeller working together.

Figure 7 shows results from tilting the propeller by 20 degrees clockwise, with the flap deactivated. The separation bubble is larger, but the lift force is greater than when the propeller is perpendicular to the wing chord. This is likely due to the greater downward component caused by the propeller's orientation.

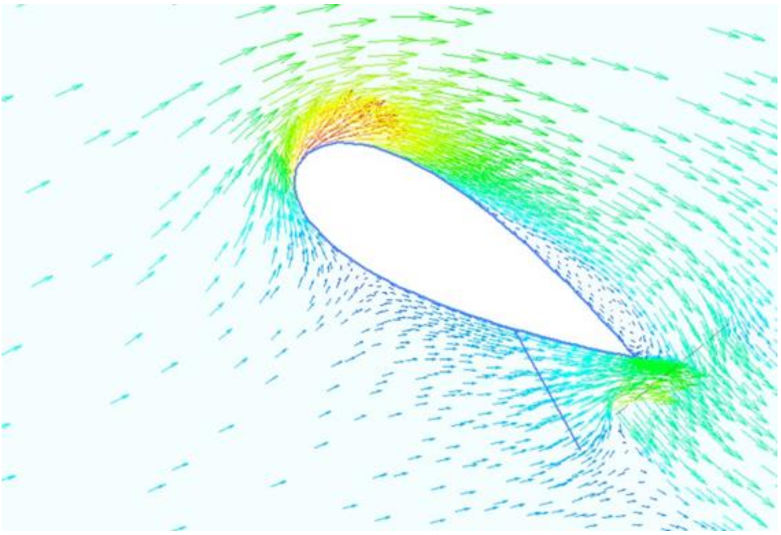

Figure 7. The propeller is tilted back 20 degrees from the perpendicular to the chord line.

Figure 8 shows that increasing the tilted propeller exit velocity from 10 m/s to 20 m/s appears to eliminate or greatly reduce flow separation on the wing.

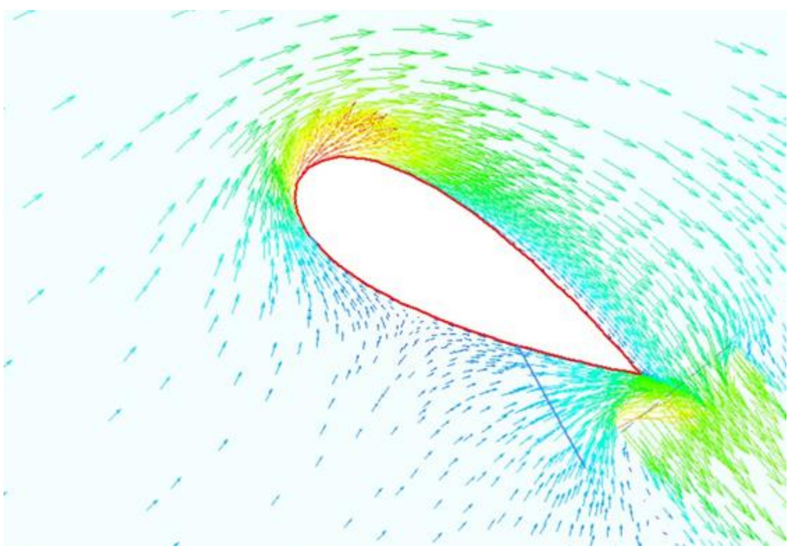

Figure 8. Tilted propeller with propeller exit speed of 20 m/s.

2-dimensional CFD Calculation of Lift, Drag and Power to turn propellers

EasyCFD [5, 6] is an educational 2-dimensional CFD tool that is ideal for preliminary analyses, permitting rapid simulation set-up. The SST turbulence model was used with a mesh size of about 20,000 cells, a size known to give reasonable results for calculation of an airfoil lift coefficient with non-separating flow [7, 8]. Trials with finer meshes in this report resulted in very small changes in the results, indicating the mesh size was appropriate.

Extension of 2-D (2-dimensional) results to real 3-D wings can be accomplished through a well-established procedure for wings under normal use, accounting for the vortices shed from the wingtips of real wings. These vortices have the effect of reducing the slope of the lift vs. angle of attack plot, as well as increasing the drag force of the 2-D wing. For 3-D wings with large aspect ratios (a tall and thin wing; aspect ratio is calculated here by wingspan/chord), the lift and drag values approach those of 2-D wings [2] and the induced drag tends to zero.

To calculate power required to run the propellers, we use the Bernoulli equation (with a work term added) to analyze the flow through the control volume shown in Figure 9, assuming frictionless, steady flow.

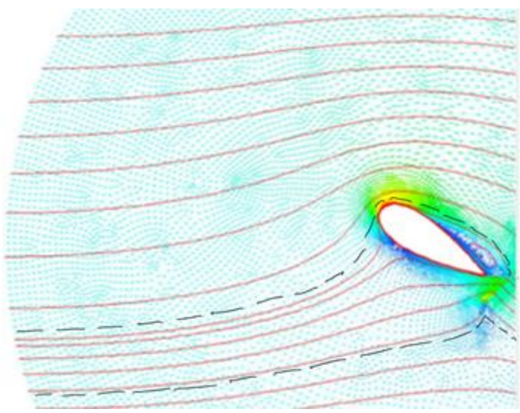

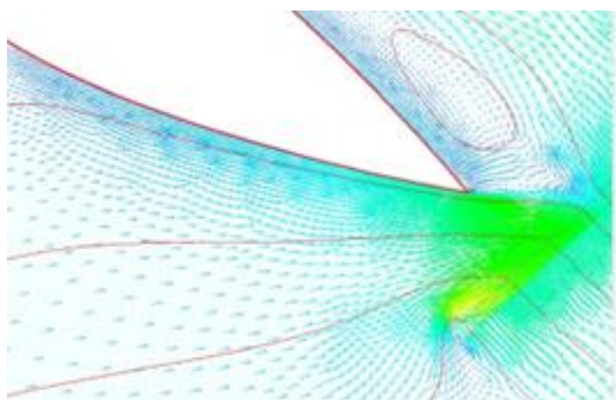

Figure 9. At left, control volume analyzed is depicted by dashed lines, following the path of streamlines. The flow enters at left and exits through the propeller, just aft of the wing. Figure 10, at right shows detail of the propeller (faint dashed line aft of the wing) indicating flow along streamlines.

The flow enters the control volume in Figure 9 at the left boundary and exits aft of the wing, behind the propeller. The Bernoulli equation is multiplied by the mass flow rate ($\rho\ A\ V_2$) through the propeller to calculate power input required:

$$Power = \left\{ \frac{P_1}{\rho} - \frac{P_2}{\rho} + \frac{(V_1)^2}{2} - \frac{(V_2)^2}{2} \right\} \rho\ A\ V_2\ ,$$

where P_1 and P_2 represent the pressure at the entry of the flow into the tunnel and the pressure at the propeller exit. Both of these values are obtained from the CFD results. V_1 is the apparent wind speed, and V_2 is the exit speed from the propeller, both of which are specified. ρ is the air density, considered constant, and A is the propeller area. Changes in potential energy are ignored.

It is recognized that this analysis is approximate, since friction may play an important role. The use of the Bernoulli equation applied here also requires the mass flow in and out of the control volume are equal, and that no flow occurs through the boundaries. A look at the streamlines generated by CFD in Figures 9 and 10 validates this assumption, and calculation of the mass flow rate through the inlet is approximately equal to that of the outlet at the propeller (3.8 vs 4.1 kg/s).

Early into this study, it was found that tilting the propeller clockwise by 20 degrees from the perpendicular to the chord caused a substantial increase in lift with little change in drag. For example, for a propeller perpendicular to the chord, Lift=121 N and Drag=22 N. With the propeller tilted, Lift=158 N and Drag=23N, an increase of 30% in lift, and 25% in lift-to-drag ratio. In addition, it was discovered that placing the propeller on the leading edge of the wing caused a much larger increase in the drag force than mounting the propeller on the wing trailing edge, although lift was somewhat greater. All further calculations in this study were performed using the tilted aft-mounted propeller.

Figures 11 shows lift and drag coefficients (Cl and Cd) of the NACA 0030 airfoil with tilted propellers. The wind speed is 7.2 m/s, and the propeller exit velocity is 10 m/s. Wing angle of attack is 30 degrees. Results include a) the wing acting alone b) the wing and propeller c) the wing, flap, and propeller d) the wing and propeller at 15 and 20 m/s propeller exit velocities. The wing chord is 1 m in length.

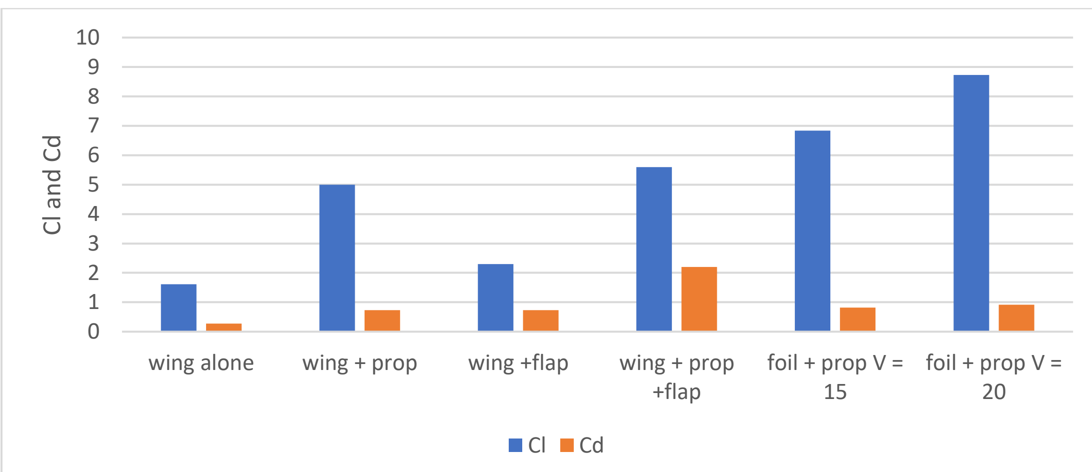

Figure 11. Lift and drag results in 2-D for NACA 0030 wing with propeller sails and flaps. The blue bars represent lift coefficient Cl, the orange bars drag coefficient Cd.

From Figure 11 we can see the following trends:

- Using the propeller always increases lift and drag
- Lift coefficients ranging from 5.1- 8.7 are possible at the propeller exit speeds and wind conditions tested, using the propeller and wing alone.
- The wing+prop+flap combination shows the highest lift coefficient at 10 m/s propeller velocity. However, the increase in lift is modest as compared to the wing+prop configuration, and the drag of the wing+prop is considerably lower. Using wing+prop+flap may not be justified.

- Increasing the propeller exit speed shows a marked increase in lift, without significant change in the drag coefficient. Of course, increasing the propeller exit velocity would require more power.

Figure 12 shows the power estimated to turn a single propeller at a variety of propeller exit velocities and diameters. The results from Figure 12 may be applied to a simple analysis involving a 15,000 CDWT vessel with a Mariner type hull and Prolss-type Dynarig sails [15]. This vessel and others were analyzed in [1] in order to determine the viability of sailing merchant ships, and preliminary designs performed, including sail areas and mast heights.

Under motor power alone (without any of the leeway drift associated with sailing vessels), the vessel would have a drag force of about 123 kN at 8 knots [1], requiring a power of 504 kW (676 HP). Using a velocity predicting program [14] with the same Mariner hull and Prolss sails, an apparent wind angle of 84 degrees, apparent wind velocity of 7 m/s and 8 knot vessel speed, the lift force from the sails (perpendicular to the apparent wind) is almost the same as the drag force on the sailing vessel (including induced drag due to vessel drift), or about 160 kN total drag [14].

With propeller sails mounted on the same vessel, a sail area of 2000 m^2 would be required to generate 160 kN of lift, assuming a lift coefficient of 5 for the propeller sails. The propeller sails are set to 20 m height (1/3 the height of the Prolss sails used in [1]) and 25 m chord, with 2.5 propellers per wing, necessitating 4 masts, for a total of eight 8-m-diameter propellers, and four 4-meter-diameter propellers. These propellers would require a total power of 295 kW (assuming 0.8 efficiency for the propellers), or about 40% of the 504 kW required to move the ship using an engine alone.

The calculations above indicate that propeller sails could be an effective method of saving fuel. It is stressed that the analysis assumed the same total drag with the propeller sails as with the Prolss sails. This can only happen if drag forces on the propeller sails can be controlled, and is discussed in the next section.

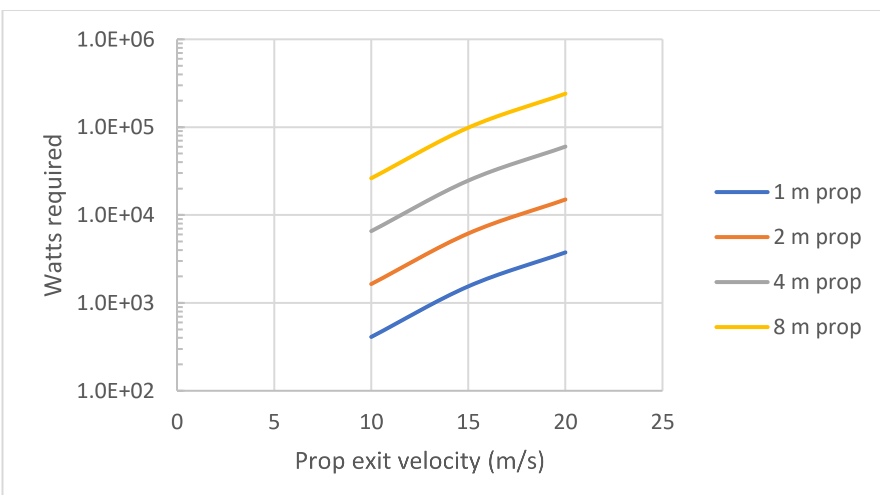

Figure 12. Power (W) required to run one propeller at a variety of exit speeds and diameters, in 7.2 m/s wind.

Induced drag, wingtip vortices and contra-vortex rotation

When the drag force on 3-D "real" wings is calculated, the force is divided into two components:

- drag due to 2-dimensional flow over the wing, with no flow along the span of the wing
- drag caused by air spilling from the high-pressure side of the wingtips, in a direction along the wingspan, causing wingtip vortices to be shed. Wingtip vortices cause an increase over the 2-D drag. This drag is referred to as induced drag or drag due to lift.

The following equations are used to calculate drag on 3-D wings [9]

$$Cd_i = \frac{(\mathrm{Cl})^2}{\pi\ e\ AR}$$

$$Cd_{total} = Cd_{2D} + Cd_i$$

$$Drag = \frac{1}{2}\ \rho\ V^2\ A\ \ Cd_{total}$$

Cd_i is the induced drag coefficient, Cd_{2D} is the 2-dimensional drag coefficient (the drag coefficient calculated using CFD), Cl is the coefficient of lift of the wing, e is the span efficiency factor (an index of how ideal a wing planform is, assumed to be 0.8 [9]), and AR is the aspect ratio of the wing (wingspan (or sail height) /chord).

One can understand from these equations the dilemma encountered when attempting to reduce mast height using high-lift devices. Increasing the lift coefficient by a factor of 5 times while reducing the mast height by a factor of 2 (which cuts the Aspect Ratio by a factor of 2 and the area by a factor of 2) causes an increase in the induced drag coefficient by a factor of 50 times, which when multiplied by the reduced area results in a drag increase of 25 times, as compared to not using the high-lift device. Under these conditions, the Cd_{2D} becomes insignificant.

But there may be a way out of this difficulty: the research in [10] shows that, if a propeller is placed at the tip of a wing, and spun in a direction counter to the wingtip vortices normally shed by wings (contra-vortex rotation), then induced drag is reduced by as much as 50%. In addition, it is well known that placing a wing or sail flush with the deck effectively doubles the aspect ratio [11]. With these two strategies, if may be possible to lower the induced drag to a level permitting use of low aspect ratio high-lift devices.

It has been known since the 1960's [12] that placing contra-vortex propellers on wingtips can reduce a wing's induced drag. In [10] the authors demonstrated that drag force can be reduced by 15% at a wing lift coefficient of 0.5, and 50% with a lift coefficient of 0.7, with propellers mounted on the leading edge of the wingtips. Similar results were found for propellers mounted on the aft portion of the wingtips in [13], with a 21 % decrease in drag for propellers set at 3 degrees lower angle of attack than the wing, at a lift coefficient of 0.3. The authors postulated that the jet from the propeller flowing into the core of the wingtip vortices dissipates the vortex.

All of these studies were limited to small angles of attack, and to the best of the author's knowledge, contra-vortex propellers have not been tested at angles of attack as large as those used in this work.

However, we can briefly analyze propeller sails mounted flush to the deck, with 26 m chord and 30 m height (this height is one half the height specified in [1] for a 15,000 CDWT pure sailing vessel with Prolss sails, and results in an aspect ratio of 1.15). If we assume similar reductions in induced drag for propeller sails at 30 degrees angle of attack as reductions documented in [10], the sail drag force is reduced to a level within 25% of the sail drag force on the Prolss ship mentioned earlier, which would place propeller sails within the realm of the possible.

Conclusions and comments

The general questions that must be answered in future work can be summarized as: (a) Are propeller sails effective at generating lift from wing-sails? (b) Can induced drag associated with low aspect ratios and high lift coefficients be brought under control? (b) Can lift be generated without excessive power? (c) Can the distributed propellers be practical in rough weather and in cargo-handling environments?

The following specific observations are noted:

1) Mounting propellers on the aft end of a NACA 0030 rigid wing-sail at a 30 degree angle of attack appears to produce lift coefficients of 5 and higher.
2) Increasing the propeller exit speed increases the coefficient of lift, with a small increase in drag and an increase in required power.
3) A combination of propeller and flap on the wing produced the highest lift coefficient, with a very large increase in drag force. A better option may be the wing and propeller combination, with a lift coefficient not too far below that of the propeller and flap, but with a much lower drag coefficient.
4) Placing the propeller on the aft end of the wing produces somewhat less lift, but with considerably less drag than mounting the propellers forward of the wing.
5) The use of contra-vortex wingtip propellers may reduce the induced drag on propeller sails as well as on Flettner rotors and suction sails. To increase the effective aspect ratio and further reduce induced drag, the wing sails should be mounted flush with the deck.
6) Based on the preliminary analysis conducted here, the use of propeller sails in 7 m/s winds could result in greater than 50% fuel savings for a 15,000 CDWT vessel moving at 8 knots, as compared to the same vessel under engine power alone.
7) The results of this preliminary analysis must be verified by laboratory or field experiments, as simplifying assumptions were used that could have significant effects on the results, such as 2-dimensional flow using CFD and the use of a linear actuator disk as a propeller. CFD products are known to be unreliable when analyzing separating flows, and contra-vortex propellers have not, to the author's knowledge, been tested at the high angles of attack proposed in this work.
8) An unexplored question that might be addressed in further research is the ideal proportion of total mechanical thrust produced by the wing propellers, with respect to the ship's normal propellers. There may be benefits to assigning a large fraction of the mechanical thrust to the wing propellers. For example, the wing propellers could be used to counter heeling and drift

normally experienced by sailing vessels, while simultaneously using the sails to extract energy from the wind. Wing-mounted propellers on a multi-mast ship could also be used to replace or augment bow and stern thrusters. In addition, the complete elimination of the ship's underwater propellers, if possible, could result in a reduction in ship construction costs.

REFERENCES

[1] Feasibility of sailing ships for the American merchant marine; J. Woodward, R. Beck, B. Scher and C. Cary, Report #168, Feb 1975, University of Michigan Department of Naval Architecture and Marine Engineering, report to the U.S. Maritime Administration

[2] Theory of Wing Sections; Abbot and von Doenhoff, Dover Books, 1959

[3] A review of the Magnus effect in aeronautics; Jost Seifert, Progress in Aerospace Sciences 55 (2012) 17–45

[4] Foundation Cousteau and windship propulsion, 1980-1985 System Cousteau-Pechiney; Bertrand CHARRIER Jacques CONSTANS Jacques-Yves COUSTEAU Abdallah DAIF Lucien MALAVARD Jean-Luc QUINIO, Journal of Wind Engineering and Industrial Aerodynamics, 20 (1985) 39--60 Elsevier Science Publishers B.V., Amsterdam

[5] EasyCFD http://www.easycfd.net/

[6] A Versatile Software Tool for the Numerical Simulation of Fluid Flow and Heat Transfer in Simple Geometries, by A.M.G. Lopes, Computer Applications in Engineering Education, 18(1):14 – 27, DOI:10.1002/cae.20230

[7] Tutorial: www.easycfd.net/index_files/Page377.htm

[8] EasyCFD User's Manual António Manuel Gameiro Lopes 2020

[9] Introduction to flight; J.D. Anderson, 5th edition, McGraw-Hill 2005

[10] Wingtip-mounted propellers: aerodynamic analysis of interaction effects and comparison with conventional layout; Tomas Sinnige, Tom Stokkermans, Nando van Arnhem, Georg Eitelberg, Journal of Aircraft, November 2018

[11] Principles of Yacht Design; L. Larsson, R. Eliasson, M. Orych, 4th edition, McGraw-Hill

[12] Effects of wingtip-mounted propeller on wing lift, induced drag and shed vortex pattern; M. Snyder, Ph.D. thesis, Oklahoma State University, May, 1967

[13] Evaluation of installed performance of a wingtip mounted pusher Turboprop on a semispan wing; James Patterson and Glynn Bartlett, NASA Technical Paper 2739, Langley Research Center, 1987

[14] OpenVPP: An open source dynamic velocity-prediction program for cargo sailing vessels, Journal of Merchant Ship Wind Energy, Sergio Perez, January 2023, www.jmwe.org

[15] Wind tunnel tests for a six-masted sailing vessel by Prölss: Translation of B. Wagner's "Windkanalversuche für einen sechsmastigen Segler nach Prölss"; L.A. Ribarov, May 2022, Journal of Merchant Ship Wind Energy, www.jmwe.org